2008 8th IEEE-RAS International Conference on Humanoid Robots
December 1 ~ 3, 2008 / Daejeon, Korea

Pattern Generation for Bipedal Walking on Slopes and Stairs

Weiwei Huang, Chee-Meng Chew, Yu Zheng, Geok-Soon Hong

Department of Mechanical Engineering
National University of Singapore, Singapore
{huangweiwei, mpeccm, mpezy, mpehgs}@nus.edu.sg,

***Abstract*— Uneven terrain walking is one of the key challenges in bipedal walking. In this paper, we propose a motion pattern generator for slope walking in 3D dynamics using preview control of zero moment point (ZMP). In this method, the future ZMP locations are selected with respect to known slope gradient. The trajectory of the Center of Mass (CoM) of the robot is generated by using the preview controller to maintain the ZMP at the desired location. Two models of slope walking, namely upslope and downslope, are investigated. Continuous walking on slopes with different gradients is also studied to enable the robots to walk on uneven terrains. Since staircase walking is similar to slope walking, the slope walking trajectory generator can also be applied to the staircase walking. Simulation results show that the robot can walk on many types of slopes and stairs by using the proposed pattern generator.**

I. Introduction

Humanoid robots have received much attention recently. Many advanced robots such as ASIMO, HRP, and HUBO have shown us robust walking behaviors in human environment. Since uneven terrain is common in human environment, uneven terrain walking is one of the important tasks in bipedal robot research. This motivates us to achieve dynamic walking on the slope and staircase.

To achieve slope walking, Chew et al. proposed an intuitive approach [1]. Kajita et al.[2] developed a simple control method based on Linear Inverted Pendulum Mode to control a bipedal walking on ground and rough terrain. Other interesting work on slope walking can be found in [3][4][5][6]. In addition, inspired by biological experiment, Taga et al.[7] investigated the use of CPG to control the walking of a simulated humanoid on slope terrain. However, those algorithms are all based on 2D experiment. None of them have been extended to 3D environment in which the dynamics is much more complex.

To investigate the stability of human walking, Vukobratovic[8] proposed a concept called Zero Moment Point (ZMP). Although the ZMP algorithm and its variants have been used to realize stable walking for many bipedal robots, they are somewhat complex and computationally intensive since the full dynamics of the robot is considered. Kajita et al.[9] proposed a cart-table model to simplify the ZMP calculation. He introduce a controller named preview controller, which uses foot placement information as an input to generate a walking gait. By utilizing the future foot place information, the gait generator produces a robust walking trajectory for the robot walking on the flat terrain. Park and Youm[10] further improved the model by taking into account the effect of horizontal angular momentum. Although the model shows a good performance on the flat terrain walking, it was not extended to slope and staircase walking. To do this, Kajita et al. [9] introduced another constraint to decouple the frontal and sagittal motion and achieved spiral stair walking. However, the detail of this method was not disclosed.

In this paper, we present a new method for slope walking based on cart-table model and preview controller. When CoM moves parallel with the slope, the frontal and sagittal motion can be decoupled. Here, no additional constraint is required. Assume that the slope gradient is known, the model could generate the walking trajectories based on the gradient and desired step length. In the real environment, the slope gradient may not be constant. Thus, we also analyze the case that the robot walks continuously on slopes with different gradients. Using simulation, we have shown that the robot can walk from flat ground to slope with different gradients and then walk down to flat ground successfully. The detail of the proposed method is presented in Section III. The simulation results are included in Section IV.

II. Cart-table model with preview controller[9]

A. Cart-table model in 2D

By combining the ZMP approach and the inverted pendulum based approach, Kajita et al.[9] introduced the cart-table model to simplify the ZMP based control. Fig. 1 shows an example of cart-table model in 2D plane. The robot is assumed to be a point mass. When the robot moves forward, the height of the center of mass (CoM) is assumed to be constant.

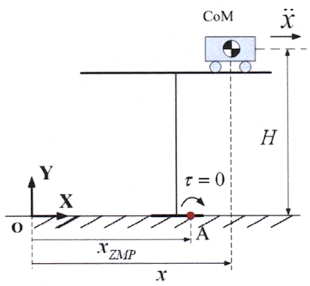

Fig. 1. An example of cart-table model[9]

978-1-4244-2822-9/08/$25.00 ©2008 IEEE

The overall torque at the ZMP point(point A in Fig. 1) is:

$$\tau = mg(x - x_{ZMP}) - m\ddot{x}H = 0 \quad (1)$$

From (1), the ZMP position can be calculated by

$$x_{ZMP} = x - \ddot{x}\frac{H}{g} \quad (2)$$

Equation (2) shows that given a trajectory of CoM, ZMP trajectory can be calculated. On the other hand, given a ZMP trajectory, it is also possible to determine the CoM trajectory of the robot. To ensure that the resultant CoM trajectory tracks the desired ZMP trajectory, a new variable is defined as $\frac{d}{dt}\ddot{x} = u$ which is the changing rate of CoM acceleration. For the state $\mathbf{x} = \{x_{CoM}; \dot{x}_{CoM}; \ddot{x}_{CoM}\}$, (2) can be transformed into the state equation:

$$\begin{aligned} \dot{\mathbf{x}} &= A\mathbf{x} + Bu \\ x_{ZMP} &= C\mathbf{x} \end{aligned} \quad (3)$$

$$A = \begin{bmatrix} 0 & 1 & 0 \\ 0 & 0 & 1 \\ 0 & 0 & 0 \end{bmatrix} B = \begin{bmatrix} 0 \\ 0 \\ 1 \end{bmatrix} C = \begin{bmatrix} 1 & 0 & -\frac{H_{CoM}}{g} \end{bmatrix}$$

A robust controller based on preview control[11] was designed to track the desired ZMP trajectory.

$$u(k) = -G_I \sum_{i=0}^{k} e(i) - G_X \mathbf{x}(k) - \sum_{i=1}^{N_L} G_P(i) x_{ZMP}^{ref}(k+i) \quad (4)$$

where N_L is the number of reference ZMP values in the future, $e(i) = x_{ZMP}^{ref}(i) - x_{ZMP}(i)$ and G_I, G_X and G_P are the gain factors. The detailed calculation of these factors can be found in Katayama's paper [11]. Fig. 2 shows the general structure of the pattern generator.

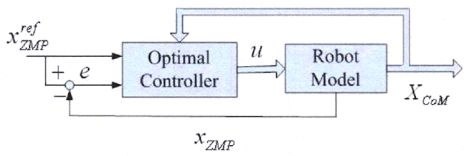

Fig. 2. Pattern generator structure to track desired ZMP trajectory

B. Cart-table model in 3D

As for cart-table model in 3D plane, Kajita et al.[2] have analyzed the dynamic of 3D linear inverted pendulum model and successfully decoupled it into two 2D linear inverted pendulum models. Fig. 3 depicts an inverted pendulum model in (X,Y,Z) plane where τ_x and τ_z are the actuator torques about X and Z axes, respectively. The dynamic equations about X and Z axes are

$$\tau_x + mgz = m(y\ddot{z} - z\ddot{y}) \quad (5)$$

$$\tau_z - mgx = m(-y\ddot{x} + x\ddot{y}) \quad (6)$$

where m is the mass of the inverted pendulum. Assume that the robot walks with constant height H. This means that $\ddot{y} = 0$.

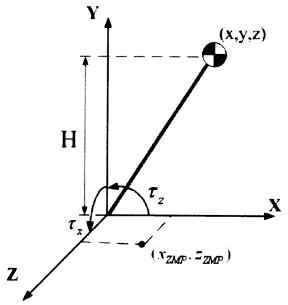

Fig. 3. 3D inverted pendulum model

Since $\tau_x = -mgz_{ZMP}$ and $\tau_z = mgx_{ZMP}$[9], from (5) and (6) we obtain

$$z_{ZMP} = z - \ddot{z}\frac{H}{g} \quad (7)$$

$$x_{ZMP} = x - \ddot{x}\frac{H}{g} \quad (8)$$

Thus the 3D model has been decoupled into two separated 2D models in the flat terrain. However, in the slope terrain walking, the height of CoM is not constant. To solve this problem, Kajita et al.[2] assumed that the height of the CoM will move within the constraint plane given by

$$y = ax + bz + H \quad (9)$$

Substituting (9) to (5) and (6) yields

$$\tau_x + mgz = m\ddot{z}H + m(x\ddot{z} - z\ddot{x})a \quad (10)$$

$$\tau_z - mgx = -m\ddot{x}H + m(x\ddot{z} - z\ddot{x})b \quad (11)$$

To decouple them, another constraint $x\ddot{z} - z\ddot{x} = 0$ must be satisfied. However, no information was provided on how to satisfy this constraint. In the next section, we propose our method to remove this constraint problem.

III. Models for Uneven Terrain Walking

A. Method for Upslope and Downslope Walking

It is difficult to decouple the frontal and sagittal motion when the robot walks on the slope. Here we attach a new frame O_1 to the slope(see Fig.4). We have assumed that the slope has constant height along Z_1 direction and robot is walking along X_1 direction. The CoM of the robot is assumed to move parallel with the slope. In this case, the frontal and sagittal motion can be decoupled in this new frame. No additional constraint is required.

Fig. 4 shows the cart-table model for upslope walking. The dynamic equations about Z_1 and X_1 axes are

$$\tau_z - mg\cos\theta x_1 + mg\sin\theta y_1 = m(-y_1\ddot{x}_1 + x_1\ddot{y}_1) \quad (12)$$

$$\tau_x + mg\cos\theta z_1 = m(y_1\ddot{z}_1 - z_1\ddot{y}_1) \quad (13)$$

In the new frame O_1, $y_1 = H$ and $\ddot{y}_1 = 0$. Since $\tau_z = mg\cos\theta x_{1(ZMP)}$ and $\tau_x = -mg\cos\theta z_{1(ZMP)}$ in this new

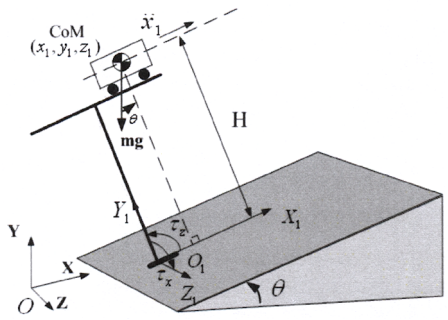

Fig. 4. Cart-table model for upslope walking

frame, from (12) and (13) we attain

$$x_{1(ZMP)} = x_1 - \frac{H}{g\cos\theta}\ddot{x}_1 - H\tan\theta \quad (14)$$

$$z_{1(ZMP)} = z_1 - \frac{H}{g\cos\theta}\ddot{z}_1 \quad (15)$$

The frontal and sagittal planes on the slope are decoupled with no additional constraint.

The preview control generator can be used to generate the desired CoM trajectory. For the state $\mathbf{x_1} = \{x_1, \dot{x}_1, \ddot{x}_1\}$ where $\frac{d}{dt}\ddot{x}_1 = u_x$, the state equations of the sagittal plane is

$$\begin{aligned} \dot{\mathbf{x}}_\mathbf{1} &= A_x\mathbf{x_1} + B_x u_x \\ x_{1(ZMP)} &= C_x\mathbf{x_1} + D_x \end{aligned} \quad (16)$$

$$A_x = \begin{bmatrix} 0 & 1 & 0 \\ 0 & 0 & 1 \\ 0 & 0 & 0 \end{bmatrix} B_x = \begin{bmatrix} 0 \\ 0 \\ 1 \end{bmatrix}$$

$$C_x = \begin{bmatrix} 1 & 0 & -\frac{H}{g\cos\theta} \end{bmatrix} D_x = -H\tan\theta$$

For the state $\mathbf{z_1} = \{z_1, \dot{z}_1, \ddot{z}_1\}$ where $\frac{d}{dt}\ddot{z}_1 = u_z$, the state equations of the frontal plane is

$$\begin{aligned} \dot{\mathbf{z}}_\mathbf{1} &= A_z\mathbf{z_1} + B_z u_z \\ z_{1(ZMP)} &= C_z\mathbf{z_1} \end{aligned} \quad (17)$$

$$A_z = \begin{bmatrix} 0 & 1 & 0 \\ 0 & 0 & 1 \\ 0 & 0 & 0 \end{bmatrix} B_z = \begin{bmatrix} 0 \\ 0 \\ 1 \end{bmatrix} C_z = \begin{bmatrix} 1 & 0 & -\frac{H}{g\cos\theta} \end{bmatrix}$$

Therefore, we attain the reference CoM trajectory in frame O_1 and change it to the desired CoM trajectory in frame O with the transformation matrix Φ from frame O_1 to frame O(Fig. 5). Fig. 6 gives an example of the CoM trajectory generated by the generator when it tries to track the desired reference ZMP trajectory. The same strategy can also be used in staircase walking as it can be considered as a special case of slope walking where the swing foot lands on a flat plane instead of a slope.

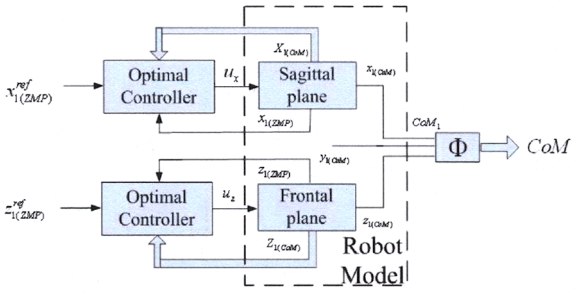

Fig. 5. Pattern generator to track ZMP trajectory for slope walking

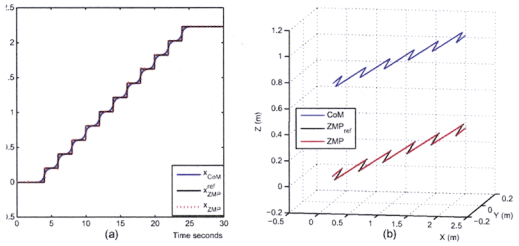

Fig. 6. An example of CoM trajectory for upslope walking (a) CoM trajectory in X direction (b) CoM trajectory in 3D plane

The strategy of upslope walking can also be applied to downslope walking. Fig. 7 shows the model for downslope walking. The ZMP equations for downslope walking are

$$x_{1(ZMP)} = x_1 - \frac{H}{g\cos\theta}\ddot{x}_1 + H\tan\theta \quad (18)$$

$$z_{1(ZMP)} = z_1 - \frac{H}{g\cos\theta}\ddot{z}_1 \quad (19)$$

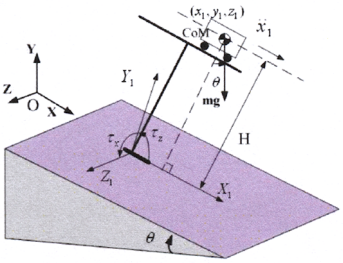

Fig. 7. Cart-table model for downslope walking

B. Continuous Walking on Slope with Different Gradients

For the pattern generators mentioned above, the slope gradient is included in the models. When the slope gradient changes, the model to generated the CoM trajectories will be different. In the human environment, an uneven terrain may be composed of slopes with different gradients. Then a method of combining several pattern generator models is needed to enable robots to continuously walk on various slopes.

When the robot walks from one slope gradient to another gradient, the model to generate the CoM trajectories will shift from one model to another model. This may cause the walking trajectories discontinuous. To make this shift successful, the trajectories should be smooth and continuous when the model shifts. Fig. 8 shows an example of a robot walking from a flat terrain to a slope.

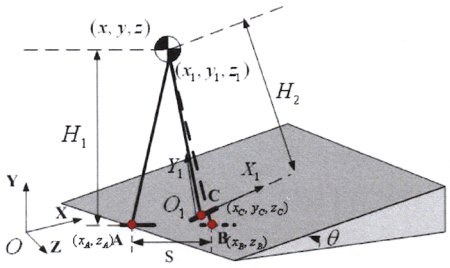

Fig. 8. Walking from flat terrain to slope

In Fig. 8, point C is the desired ZMP location after the foot touches the slope. A new frame O_1 is attached to point C for the slope walking. The coordinate transformation of a point between the two frames is given by

$$x_1 = (x - x_c)\cos\theta + (y - y_c)\sin\theta \quad (20)$$

$$y_1 = -(x - x_c)\sin\theta + (y - y_c)\cos\theta \quad (21)$$

$$z_1 = z - z_c \quad (22)$$

where $\{x_c, y_c, z_c\}$ is the position of point C, namely the origin of frame O_1, in frame O.

However, point C cannot be used as the future ZMP reference for flat terrain model as it is on the slope. Here, we create an imaginary reference ZMP location B on the flat terrain. The CoM will move forward according to the imaginary reference ZMP B, while the foot is actually placed at point C. The location of B is designed to ensure that the ZMP location will shift to point C when the foot touches the slope.

The step distance between A and B is S. If the swing foot could move to point B, the position of the CoM$\{x, y, x\}$ is: $x = x_B - \frac{S}{2}; y = H_1; z = 0$ when the foot touches B. Then, the ZMP location would shift to B once the foot touches B. According to (2), the acceleration of CoM at that moment should be

$$\ddot{x} = \frac{g}{H_1}(x - x_B) = -\frac{gS}{2H_1} \quad (23)$$

However, the foot is actually at point C on the slope. In this case, the CoM position is still taken to be the one obtained with respect to the imaginary location B in the flat terrain model. The CoM position$\{x_1, y_1, z_1\}$ in frame O_1 can be calculated by (20)-(22). In frame O_1, $\ddot{x}_1 = \ddot{x}cos\theta + \ddot{y}sin\theta = \ddot{x}cos\theta$. If the ZMP location in frame O_1 could be at point C, the robot will be stable when shifting from one model to another. The ZMP equation at point C in frame $O_1$is $x_{zmp} = x_1 - \ddot{x}_1\frac{y_1}{g}$. Since C is the origin of frame O_1, $x_{zmp} = 0$.

$$x_1 = \ddot{x}_1\frac{y_1}{g} = -\frac{gScos\theta y_1}{2H_1} \quad (24)$$

Here, x_1 and y_1 can be computed by (20) and (21). Therefore, to make the robot stable when it walks from flat terrain to slope, the last imaginary step length of flat terrain walking should satisfy

$$S = -\frac{2H_1x_1}{y_1cos\theta} \quad (25)$$

To keep the trajectory continuous, the constant height of the new model H_2 should be equal to y_1.

The same idea can also be applied to the case of different types of slopes. Fig. 9 shows an example of CoM trajectory generator by pattern generator of four models when the robot starts from a flat terrain, walks through 10^o and 20^o slopes successively, and finally arrives at another flat terrain.

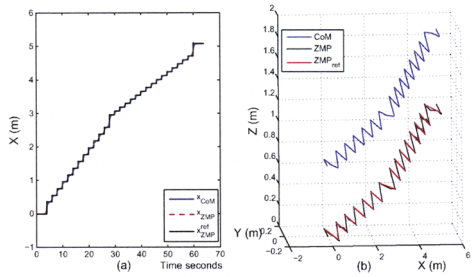

Fig. 9. An example of CoM trajectory for 10^o and 20^o slope walking

IV. Simulation Experiments

A. Setup of Simulation Experiments

The simulation software used here is Webots, which allows users to conduct realistic physical and dynamical simulation of robots in the 3D virtual environment. The simulated robot is about 175cm high and weighs 75 kg. It has 42 DoFs (7 on each leg, 6 on each arm, 6 on each hand, 2 on the waist and 2 on the neck).The mass distribution of the robot is listed in Table I. A schematic diagram of the robot is shown in Fig. 10. To measure the real ZMP location during the walking, four force sensors are placed on each foot of the robot. Using the force sensors can avoid the requirement on knowing the accurate model of the robot and is an effective way to measure the actual ZMP location[12].

B. Slope and Stair Walking

To test the effectiveness of our controller, we conduct four simulations(upslope walking, downslope walking, stair walking and transition walking from 10^o to 20^o slopes). The actual ZMP location is measured and compared with the reference ZMP trajectories.

Fig. 11 shows the CoM trajectory for the upslope walking generated by (16) and (17). In the flat terrain walking, the

TABLE I

PARAMETERS OF THE SIMULATED ROBOT

	Mass(Kg)	Length(mm)
Head and Neck	4	220
Trunk	24	580
Upper Arm	3.5x2	320
Lower Arm	2x2	280
Hand	1.8x2	160
Thigh	8x2	420
Shank	6x2	420
Foot	2.2x2	310(Height 110)

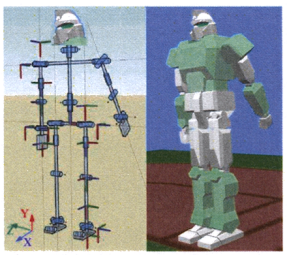

Fig. 10. Schematic diagram of the simulated robot

reference ZMP is usually at the center of the support leg to enlarge the stability margin. In the upslope walking, leaning the body forward helps the slope walking. To achieve this, we shift the ZMP point a little forward. Since the future foot location is known, the desired foot trajectories are generated using an 8th degree polynomial. The reference joint angles for the robot can be derived through inverse kinematics. Fig. 12 shows the stick diagram of the walking on a 10^o slope in sagittal plane. The resultant ZMP trajectories are shown in Fig. 13. The up, low, left and right limits indicate the stability margins which are the foot projections on the XZ plane. As shown in Fig. 13, the actual ZMP trajectories are different from the reference ZMP trajectories because of the dynamic difference between robot and cart-table model.

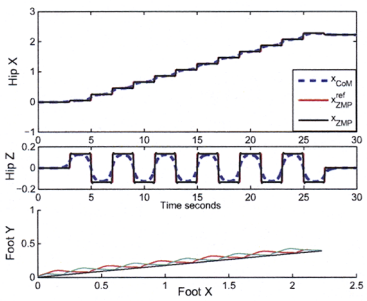

Fig. 11. Generated CoM trajectories for upslope walking and planned foot trajectories

As for the downslope walking, we plan the ZMP trajectory a little backward. It will cause the robot to lean backward for downslope walking. The CoM trajectories are generated by (18) and (19). Fig. 14 shows the stick diagram of downslope

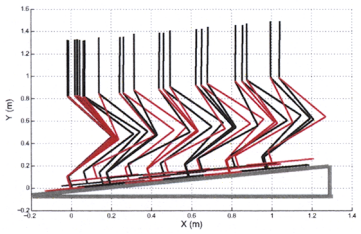

Fig. 12. Stick diagram of upslope walking on 10 degrees of slope in sagittal plane

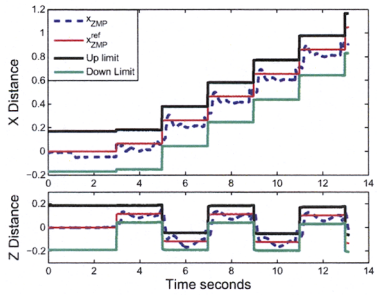

Fig. 13. The resultant ZMP trajectories of upslope wakling

walking in sagittal plane. The resultant ZMP trajectories are shown in Fig. 15. Compared with the upslope walking, the actual ZMP trajectories of downslope walking are closer to the reference ZMP trajectories. Here, the step length is shorter than that of the upslope walking. Because the swing leg motion is ignored by the cart-table model, when the step length is large, it will affect the resultant ZMP location of the robot.

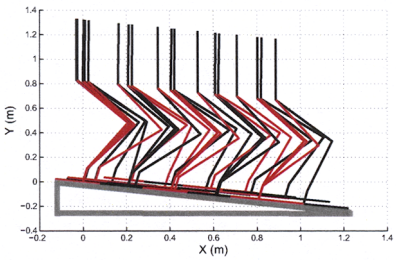

Fig. 14. Stick diagram of downslope walking on 10 degrees of slope in sagittal plane

Since the staircase walking could be considered as a special case of slope walking while the feet touch the flat ground, we adopt the same strategy as that in the slope walking for the staircase walking. Figs. 16 and 17 show the snapshots of the up staircase walking and the resultant ZMP trajectories, respectively. In the staircase walking, the step length is 375mm which is quite long in comparison with slope walking, so that the swing leg motion has greater effect on the ZMP location. We have also conducted the walking simulation on an uneven

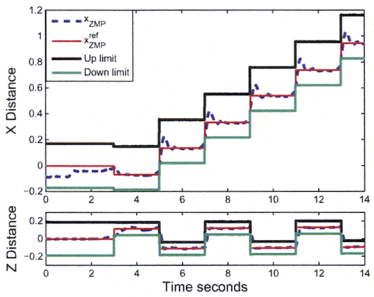

Fig. 15. The resultant ZMP trajectories of downslope wakling

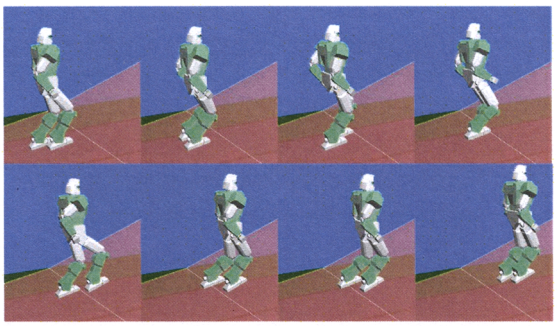

Fig. 18. Snapshots of continuously walking on 10^o and 20^o slopes

terrain composed of different types of slopes. The robot can walk from a flat terrain, pass through 10^o and 20^o slopes, and reach another flat terrain. The snapshots of continuous walking between the 10^o and 20^o slopes are shown in Fig. 18.

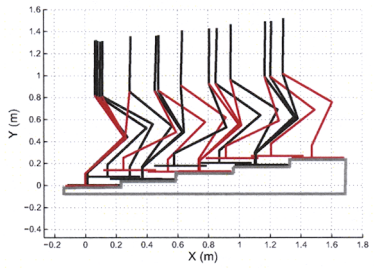

Fig. 16. Stick diagram of stair walking in sagittal plane (stair height=65mm and stair length=375mm)

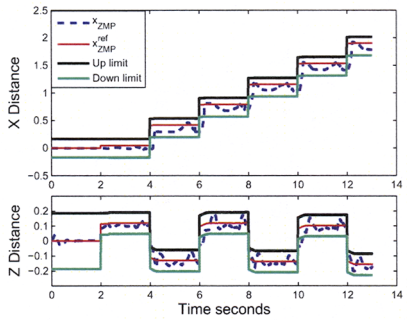

Fig. 17. The resultant ZMP trajectories of up stair walking

V. Conclusion and Future Work

We proposed an intuitive method for slope and staircase walking based on cart-table model. No additional constraint is needed to decouple the frontal and sagittal motions. Three kinds of slope walking are studied: upslope walking, downslope walking and continuous walking on slope with different gradients. Dynamic simulation results show that the robot can walk on many kinds of uneven terrains by using the CoM trajectories generated by the proposed pattern generator. In the simulation, the slope gradient is assumed to be known. In the real implementation, we may design some methods to detect the slope gradient, such as using a distance sensor to approximate the slope gradient, then using the force torque sensor on the foot to make the foot level with the slope, thus knowing the exact slope gradient.

References

[1] C.-M. Chew, J. Pratt, and G. Pratt, "Blind walking of a planar bipedal robot on sloped terrain," in *Proceedings of the 1999 IEEE International Conference on Robotics and Automation*, Detroit, Michigan, May 1999, pp. 381–386.

[2] S. Kajita, O. Matsumoto, and M. Saigo, "Real-time 3d walking pattern generation for a biped robot with telescopic legs," in *Proceedings of the 2001 IEEE International Conference on Robotics and Automation*, Seoul, Korea, May 2001, pp. 2299–2306.

[3] T. Erez and W. D. Smart, "Bipedal walking on rough terrain using manifold control," in *Proceedings of the 2007 IEEE/RSJ International Conference on Intelligent Robots and Systems*, San Diego, CA, 2007, pp. 1539–1544.

[4] J. K. Hodgins and M. H. Raibert, "Adjusting step length for rough terrain locomotion," *IEEE TRANSACTIONS ON ROBOTICS AND AUTOMATION*, vol. 7, no. 3, pp. 289–298, 1991.

[5] M. Ogino, H. Toyama, and M. Asada, "Stabilizing biped walking on rough terrain based on the compliance control," in *Proceedings of the 2007 IEEE/RSJ International Conference on Intelligent Robots and Systems*, San Diego, CA, 2007, pp. 4047–4052.

[6] L. Yang, C.-M. Chew, T. Zielinska, and A.-N. Poo, "A uniform biped gait generator with offline optimization and online adjustable parameters," *Robotica*, vol. 25, p. 549C565, 2007.

[7] G. Taga, Y. Yamaguchi, and H. Shimizu, "Self-organized control of bipedal locomotion by neural oscillators in unpredicatable environment," *Biological Cybernetics*, vol. 65, pp. 147–159, 1991.

[8] M. Vukobratovic, A. A. Frank, and D. Juricic, "On the stability of biped locomotion," *Biomedical Engineering, IEEE Transactions on*, vol. BME-17, no. 1, pp. 25–36, 1970.

[9] S. Kajita, F. Kanehiro, K. Kaneko, K. Fujiwara, K. Harada, K. Yokoi, and H. Hirukawa, "Biped walking pattern generation by using preview control of zero-moment point," in *Proceedings of the 2003 IEEE International Conference on Robotics and Automation*, Taipei, Taiwan, 2003, pp. 1620–1626.

[10] J. Park and Y. Youm, "General zmp preview control for bipedal walking," in *Proceedings of the 2007 IEEE International Conference on Robotics and Automation*, Roma, Italy, 2007, pp. 2682–2687.

[11] T. Katayama, T. Ohki, T. Tnoue, and T. Kato, "Design of an optimal controller for a discrete-time system subject to previewable demand," *International Journal of Control*, vol. 41, no. 3, pp. 677–699, 1985.

[12] T. Ishida and Y. Kuroki, "Development of sensor system of a small biped entertainment robot," in *Proceedings of the 2004 IEEE International Conference on Robotics and Automation*, New Orleans, LA, May 2004, pp. 648–653.